Journal of Digital Imaging

Microcatheter Tip Enhancement in Fluoroscopy: A Comparison of Techniques

Akihiro Takemura, Ph.D.,[1] Kenneth R. Hoffmann, Ph.D.,[2] Masayuki Suzuki, M.D.,[1] Zhou Wang,[3] Hussain S. Rangwala,[2] Hajime Harauchi,[4] Stephen Rudin, Ph.D.,[2] and Tokuo Umeda, Ph.D.[5]

We compared three techniques for enhancement of microcatheter tips in fluoroscopic images: conventional subtraction technique (CST); averaged image subtraction technique (AIST), which we have developed; and double average filtering (DAF) technique, which uses nonlinear background estimates. A pulsed fluoroscopic image sequence was obtained as a microcatheter was passed through a carotid phantom that was on top of a head phantom. The carotid phantom was a silicone cylinder containing a simulated vessel with the shape and curvatures of the internal carotid artery. The three techniques were applied to the images of the sequence, then the catheter tip was manually identified in each image, and 100 x 100 pixel images, centered at the indicated microcatheter tip positions, were extracted for the evaluations. The signal-to-noise ratio (SNR) was calculated in each of the extracted images from which the mean value of the SNR and its standard deviation (SD) were calculated for each technique. The mean values and the standard deviations were 4.36 (SD 3.40) for CST, 6.34 (SD 3.62) for AIST, and 3.55 (SD 1.27) for DAF. AIST had a higher SNR compared to CST in almost all frames. Although DAF yielded the smallest mean SNR value, it yielded the best SNR in those frames in which the microcatheter tip did not move between frames. We conclude that AIST provides the best SNR for a moving microcatheter tip and that DAF is optimal for a temporarily stationary microcatheter tip.

KEY WORDS: Microcatheter tracking, enhancement technique, subtraction technique, signal-to-noise ratio, comparison of techniques, fluorography, endovascular intervention

INTRODUCTION

The number of endovascular interventions performed for patients with intracranial aneurysms is increasing. These interventions are less invasive than conventional surgery for intracranial aneurysms. In these endovascular interventions, coils, stents, and angioplasty balloons are transported via microcatheters. In such interventions, knowledge of the 3-dimensional (3D) position of the guide wire, the catheter tip, or the microcatheter tip relative to the vascular structures may facilitate the interventions, but determination of the 3D catheter position is difficult because the fluoroscopic image that is usually employed is 2-dimensional and noisy. Magnetic resonance imaging-based navigation systems have been investigated.[1–7] These systems can provide accurate 3D information during intervention, but they also require particular hardware; moreover, special

[1]From the School of Health Sciences, Faculty of Medicine, Kanazawa University, 5-11-80 Kodatsuno, Kanazawa, 920-0942, Japan.

[2]From the Toshiba Stroke Research Center, University at Buffalo (SUNY), 3435 Main St., Buffalo, NY 14214, USA.

[3]From the Roswell Park Cancer Institute, Elm & Carlton St., Buffalo, NY 14263, USA.

[4]From the School of Allied Health Sciences, Faculty of Medicine, Osaka University, 1-7 Yamadaoka, Suita, 565-0871, Japan.

[5]From the School of Allied Health Sciences, Kitasato University, 1-15-1 Kitasato, Sagamihara, Kanagawa, 228-8555, Japan.

Correspondence to: Akihiro Takemura, Ph.D., School of Health Sciences, Faculty of Medicine, Kanazawa University, 5-11-80 Kodatsuno, Kanazawa, 920-0942, Japan; tel: +81-76-2652538; fax: +81-76-2344366; e-mail: at@mhs.mp.kanazawa-u.ac.jp

Online publication 5 September 2006
doi: 10.1007/s10278-006-0855-6

care and devices are needed because of the magnetic field. Other investigators have proposed methods that provide 3D catheter positions by using devices which transmit electromagnetic signals to allow detection and tracking of a catheter tip in a body in conjunction with conventional x-ray angiography systems.[8,9] Image-based techniques[10] have been proposed for cardiac interventions, which align a catheter model with the catheter image in a single plane C-arm image using the projection Procrustes method.[11] Others have developed techniques to detect guide wires in fluorograms.[12–14]

We are developing an image-based system (the computer-assisted catheter guide system) to help with the navigation of catheters during an intervention for intracranial aneurysms.[15] Specifically, this system will provide image-based 3D catheter locations. However, for full automation and image fusion with this system, the catheter must be detected and tracked automatically and accurately in the images. To facilitate catheter detection, we have developed three catheter enhancement techniques. In this article, we compare these three catheter enhancement techniques in terms of the resulting signal-to-noise ratio (SNR). Evaluations were performed by using a fluoroscopic image sequence of a catheter as it was passed through a carotid phantom.

MATERIALS AND METHODS

A fluoroscopic image sequence of a catheter passing through a carotid phantom was obtained. The images were processed by using three different enhancement techniques: a conventional subtraction technique, a weighted sum of previous images, and a signal extraction technique involving local averages of local pixel values. The quality of the enhancement was evaluated by using the SNR of the resulting signal.

Fluorograms

A digital 1,024 × 1,024 × 12 bit fluoroscopic image sequence of a microcatheter passing through a carotid phantom was acquired by using the CAS-8000 V (Toshiba America Medical Systems, San Francisco, CA, USA) C-arm angiography system. The carotid phantom (Fig. 1a) consisted of a 3-mm-diameter polyethylene tube fixed in a silicone cylinder. The tube was constrained or molded to have the 3D shape and curvatures of a "typical" carotid (as determined by a neuroradiologist). The carotid phantom was positioned on a head phantom (Fig. 1b) to provide images similar to those that would be obtained during interventions, specifically to provide bony structured background in the fluorograms. The carotid phantom was set on the head phantom in a lateral position, and then those phantoms were set on the table of the angiography system. The carotid phantom was filled with a glycerin–water solution that provided smooth movement of the microcatheter. A 2.5 F (0.833 mm) Fastrack-18 Infusion microcatheter (Target, Fremont, CA, USA) was placed in the phantom and drawn back during fluoroscopic acquisition (Fig. 2). The pulsed fluorograms were acquired at 30 frames/second using 94 kVp and 50 mA. The source–surface distance was 100 cm and the magnification was 1.35. The 7-in. image intensifier mode was used (pixel size = 0.174 mm). Total acquisition time was 3.0 s. After acquisition, the 90 images were transferred to our analysis computer.

Techniques

During interventions, the catheter is guided to the site of intervention by observing the progress of the microcatheter tip under fluoroscopy. This microcatheter tip consists of a radio-opaque marker with dimensions smaller than 1 mm. The fluorograms used for guidance usually include bone background and are generally noisy because of low dose. To detect and track a microcatheter tip in fluorograms, techniques are required which suppress the bone background and provide good SNR for the catheter tip. In this article, we report on three techniques to achieve these goals: the conventional subtraction technique, the averaged image subtraction technique using temporal averaging we developed, and a double average filtering technique using spatial averaging.

Conventional Subtraction Technique

In the conventional subtraction technique (CST) (one of the simplest techniques to detect object motion between frames), the previous frame is subtracted from the current frame. Microcatheters are darker in fluorograms than background. Thus, the CST is defined as,

$$D_n(x,y) = f_{n-1}(x,y) - f_n(x,y) \quad n = 2,3,4,\ldots \tag{1}$$

$$D_n(x,y) = \begin{cases} 0 & \text{when } D_n(x,y) < 0 \\ D_n(x,y) & \text{otherwise} \end{cases} \tag{2}$$

where $D_n(x, y)$ and $f_n(x, y)$ are respectively the difference image and the image at time point or frame number n. From equation (2), we see that this technique uses a nonlinear process, i.e., if the value of $D_n(x, y)$ is negative, it is set to 0. This nonlinear process should improve SNR by eliminating signals that result from subtraction of high-intensity structures, eg, the catheter tip appearing in the $(n - 1)$ image. Using this technique, stationary structures will be removed, and moving structures will appear as brighter regions.

Averaged Image Subtraction Technique

Fluorograms are usually noisy because of the low dose. In the conventional subtraction technique, the resultant image can be noisier then the original. To reduce increment of noise and

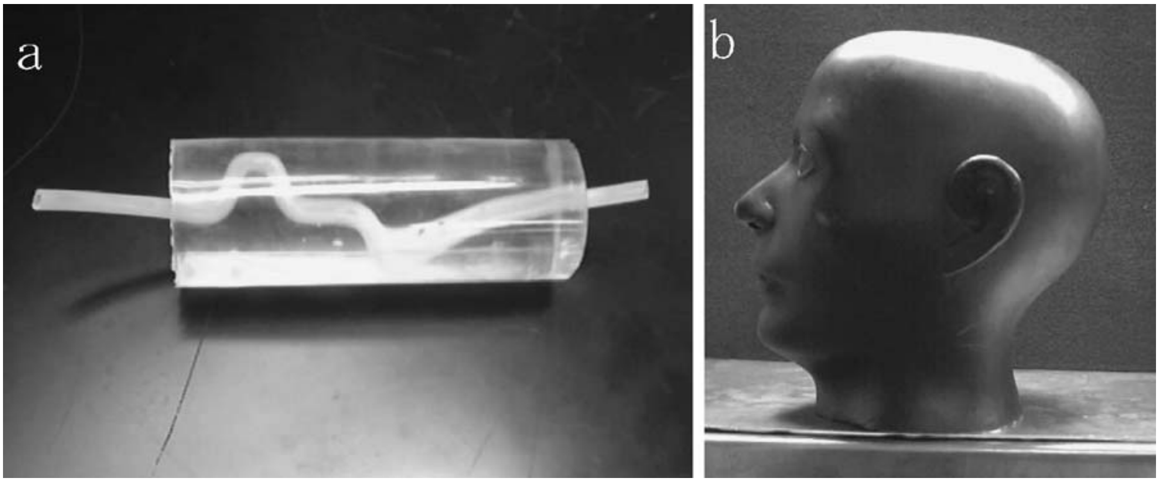

Fig 1. The carotid phantom and the head phantom. (a) A picture of the custom-made carotid phantom. The shape of the centerline of the tube fixed in silicon was based on carotid artery geometries observed by a neuroradiologist. (b) A picture of the head phantom that was used to provide structured background and scatter in the fluorograms.

to improve the SNR of the feature in the resultant image, we have developed a technique that uses an averaged image generated from the frames preceding the current frame and the current frame as a mask image. In this study, three preceding frames were used, thus, the averaged image is defined by the following equation.

$$A_n(x,y) = \frac{1}{4}\sum_{i=n-3}^{n} f_i(x,y), \quad n = 4, 5, 6, \ldots \tag{3}$$

where $A_n(x, y)$ is the averaged image, n is the frame number, and $f_i(x, y)$ is the original ith image. By using this averaged image as a mask image, the noise in the resultant images is less than that in the images generated using the CST. The equation for this technique in fluorograms in which catheters are darker than the background is thus as follows:

$$m_n(x,y) = A_n(x,y) - f_n(x,y) \qquad n = 4, 5, 6, \ldots \tag{4}$$

$$m_n(x,y) = \begin{cases} 0 & \text{when } m_n(x,y) < 0 \\ m_n(x,y) & \text{otherwise} \end{cases} \tag{5}$$

where $m_n(x, y)$is a resultant image, $A_n(x, y)$ is an averaged image generated by using equation (4), and $f_n(x, y)$ is the original ith image.

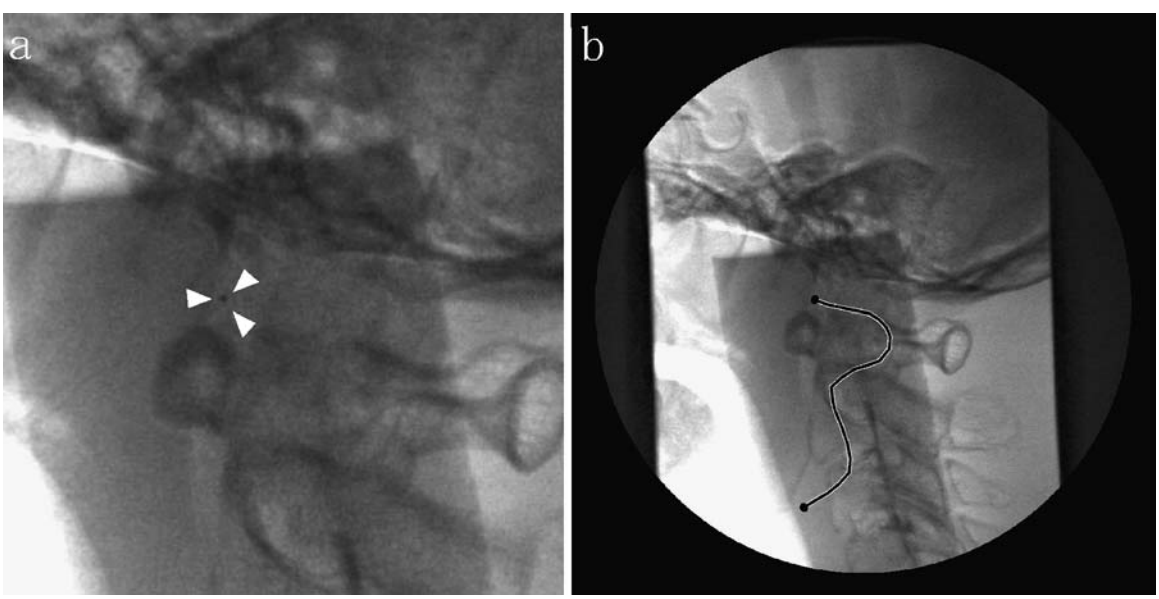

Fig 2. A microcatheter tip in a part of a magnified fluorogram and the path of the microcatheter. (a) White arrows point to the microcatheter tip. (b) The curve represents the path of the microcatheter tip in the sequence of fluorograms.

Note that this subtraction technique employs nonlinear processing similar to that used in the CST and that process could improve the SNR for this technique.

Double Average Filtering Technique

The double average filtering technique (DAF) was proposed as a preprocessing filtering for a vessel tracking technique for the coronary arteries in cine angiograms.[16] The authors indicated that the DAF did not amplify noise and did not generate artifacts that may result from conventional edge enhancement techniques. The double average filtering technique was defined as:

$$M_1(x,y) = \sum_{k=-w}^{w}\sum_{l=-w}^{w} f(x+k, y+l) \tag{6}$$

$$M_2(x,y) = \frac{\sum_{i=-w}^{w}\sum_{j=-w}^{w} f(x+i,y+j)W(x+i,y+j)}{\sum_{i=-w}^{w}\sum_{j=-w}^{w} W(x+i,y+j)} \tag{7}$$

where

$$W(x+i,y+j) = \begin{cases} 1 & \text{when} \quad f(x+i,y+j) < M_1(x,y) \\ 0 & \text{otherwise} \end{cases} \tag{8}$$

$$\tilde{f}(x,y) = \begin{cases} f(x,y) - M_2(x,y) & \text{when} \quad f(x,y) > M_2(x,y) \\ 0 & \text{otherwise} \end{cases} \tag{9}$$

where w is half-width of region of interest (ROI),$f(x, y)$ is the pixel value in the original image at coordinates (x, y), and $\tilde{f}(x,y)$ is the pixel value of final image after filtering by the DAF at coordinates (x, y). $M_1(x, y)$ is the average pixel value of all pixels in ROI, and $M_2(x, y)$ is the average pixel value of all pixels in ROI with pixel value less than $M_1(x, y)$.

Equation (9) is for the image with the signal intensity above the background. Although DAF is not only for such images, we inverted the pixel values in the fluorograms for DAF because the SNR for DAF was calculated by the same equation as for the others (see equation 10).

A size of ROI used in DAF is usually set to twice to triple the size of the feature. We investigated sizes of 5×5 up to 21×21; 15×15 yielded the best results. The size of the marker at the microcatheter tip in the fluorograms was about 5×5 pixels.

Measurement of Signal-to-Noise Ratio

To compare the three techniques described above, positions of the catheter tip in the fluorograms were first determined manually. Next, 100×100 pixel regions, centered at the indicated microcatheter tip positions were extracted from the fluorograms and processed by using the three techniques. We calculated SNR in each cropped image as:

$$SNR = \frac{\overline{S} - \overline{B}}{SD} \tag{10}$$

where, $\overline{S}$ is the mean pixel value in a 3×3 pixel region of 3×3 at the center of the extracted fluorograms (at the microcatheter

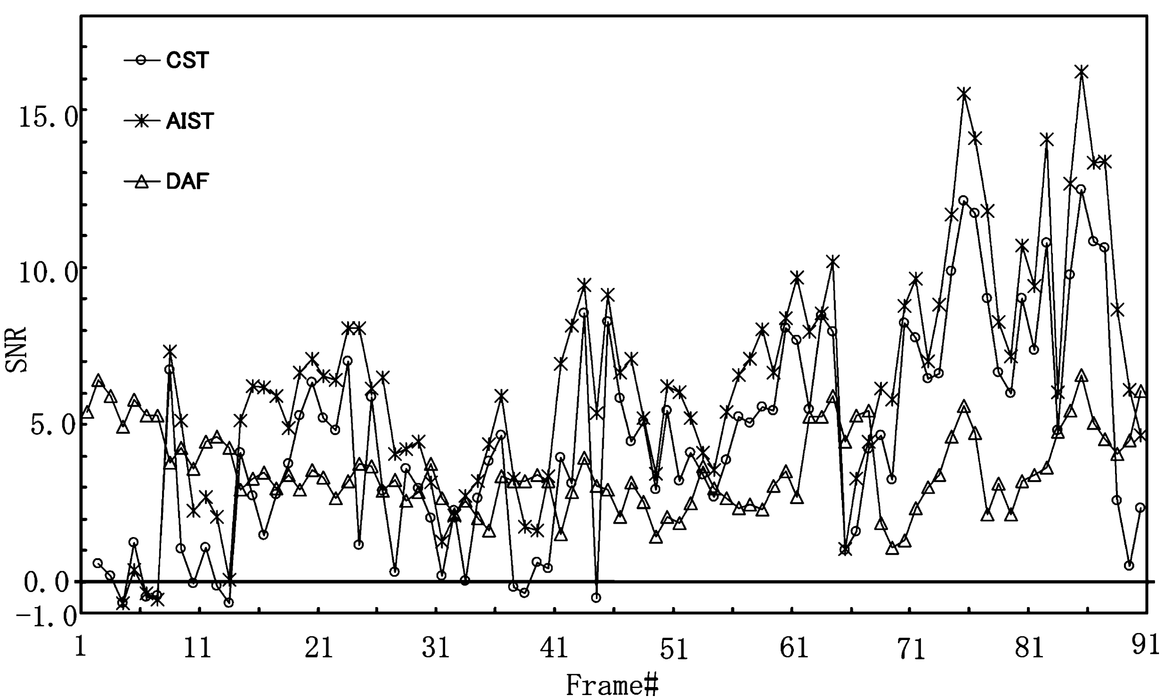

Fig 3. Variation of SNR for the three techniques. The AIST yields the best results, i.e., highest average SNR, whereas the DAF yields the lowest SD of the SNR values.

Table 1. Mean value and standard deviation of Signal-to-Noise Ratio in a sequence of fluoroscopy

Technique	CST	AIST	DAF
Mean value	4.36	6.34	3.55
Standard deviation	3.40	3.62	1.27

tip position), $\overline{B}$ is the mean value of the background, and SD is the standard deviation of background pixel values. A mean value of SNRs was also calculated from all the frames in the image sequence.

RESULTS

Variation in SNRs for each technique is shown in Figure 3, and mean values and SDs of SNRs for the three techniques are shown in Table 1. Based on mean values in Table 1, AIST has the highest overall SNR, and DAF has the lowest SNR but it also yielded the smallest SD. As shown in Figure 3, AIST and CST yielded negative SNR values in some frames, which occur when the catheter tip did not move between frames.

DISCUSSION

SNRs for AIST are similar to those for CST, but AIST showed higher SNRs than CST in almost all frames. It should be noted that AIST and CST are basically motion detectors and yield unreliable results (e.g., negative SNR values) when little or no motion occurs between frames (Fig. 4b and c). However, AIST resulted in fewer frames with negative SNR compared to CST. Thus, AIST appears to provide better enhancement than CST for microcatheter tip tracking in fluorograms.

The mean value of SNRs for DAF is less than those for AIST and CST. However, when the catheter tip does not move, DAF can provide an adequate SNR (Fig. 4d). Thus, AIST and DAF may complement each other in that AIST enhances the moving tip well and DAF enhances the stationary tip well.

When the microcatheter tip is on or near bony background, the tip is enhanced well with AIST and CST, whereas it is obscured with DAF because the local background averages (M_1 and M_2 in Double Average Filtering Technique) have lower pixel values. This is a limitation of DAF.

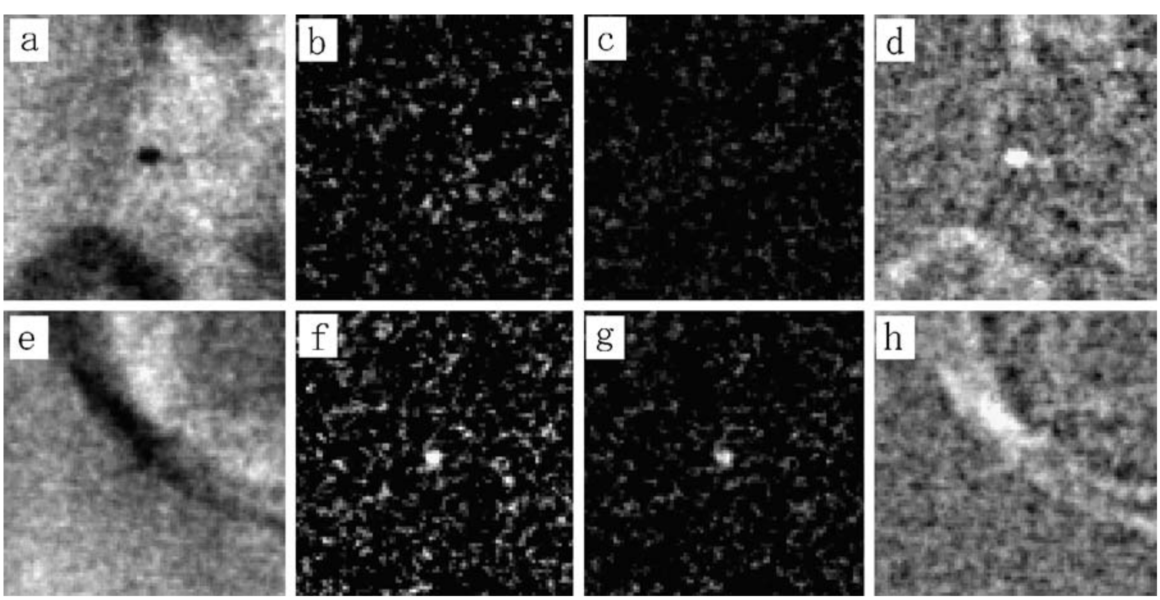

Fig 4. Examples of the original images and the images processed by the three techniques. (a) Original image of frame number seven in the sequential fluorograms. The images resulted from CST (b), AIST (c), and DAF (d). The image of the 7th frame is one of the images in which the catheter tip was not moved, so that the signals of the catheter tip in (b) and (c) have disappeared. (e) Original image of frame number 69 in the sequential fluorograms. The images resulted from CST (f), AIST (g), and DAF (h). The 69th frame is one of the images in which the catheter tip was on a bone edge. The DAF could not isolate the catheter tip signal.

In this study, fluorograms of the head phantom and the carotid phantom were obtained. We believe that addition of the carotid phantom did not affect our results, because each of the techniques estimates and subtracts out the local background. The carotid phantom introduced a slowly varying low-contrast background structure. Thus, the carotid phantom in the fluorograms probably only contributes in increasing the noise near the catheter tip.

CONCLUSIONS

Using SNR, we evaluated three techniques for tracking a microcatheter tip in fluorograms. From our results, we conclude that the averaged image subtraction technique (AIST) is the best of the three techniques for a moving microcatheter tip, and the double average filtering technique is useful for a nonmoving microcatheter tip.

ACKNOWLEDGMENTS

This research supported by a grant-in-aid for young scientists (B) (KAKENHI 15790656) of the Ministry of Education, Culture, Sports, Science, and Technology of Japan and NIH Grant numbers R01 HL52567, R01 EB 02916, R01EB002873, and R01NS43924.

REFERENCES

1. Buecker A, Neuerburg JM, Adam GB, et al.: Real-time MR fluoroscopy for MR-guided iliac artery stent placement. J Magn Reson Imaging 12:616–622, 2000
2. Dion YM, Kadi BEH, Boudoux C, et al.: Endovascular procedures under near-real-time magnetic resonance imaging guidance: an experimental feasibility study. J Vasc Surg 32:1006–1014, 2000
3. Salem RR, Ward BA, Ravikumar TS: A new peripherally implanted subcutaneous permanent central venous access device for patients requiring chemotherapy. J Clin Oncol 11:2181–2185, 1993
4. Quick HH, Ladd ME, Nanz D, et al.: Vascular stents as RF antennas for intravascular MR guidance and imaging. Magn Reson Med 42:738–745, 1999
5. Quick HH, Kuehl H, Kaiser G, et al.: Interventional MR angiography with a floating table. Radiology 229:598–602, 2003
6. Kuehne T, Saeed M, Higgins CB, et al.: Endovascular stents in pulmonary valve and artery in swine: feasibility study of MR imaging-guided deployment and postinterventional assessment. Radiology 226:475–481, 2003
7. Strother CM, Unal O, Frayne R, et al.: Endovascular treatment of experimental canine aneurysms: feasibility with MR imaging guidance. Radiology 215:516–519, 2000
8. Wittkampf FH, Wever EF, Derksen R, et al.: Accuracy of the LocaLisa system in catheter ablation procedures. J Electrocardiol 32 (Suppl 7): 12, 1999
9. Starkhammar H, Bengtsson M, Kay DA: Cath-Finder catheter tracking system: a new device for positioning of central venous catheters. Early experience from implantation of brachial portal systems. Acta Anaesthesiol Scand 34:296–300, 1990
10. Meyer SA, Wolf PD: Registration of three-dimensional cardiac catheter models to single-plane fluoroscopic images. IEEE Trans Biomed Eng 46:1471–1479, 1999
11. Hoffmann KR, Esthappan J: Determination of three-dimensional positions of known sparse objects from a single projection. Med Phys 24:555–564, 1997
12. Baert SAM, van de Kraats EB, van Walsum T, et al.: Three-dimensional guide-wire reconstruction from biplane image sequences for integrated display in 3-D vasculature. IEEE Trans Med Imag 22:1252–1258, 2003
13. Baert SAM, Viergever MA, Niessen WJ: Guide-wire tracking during endovascular interventions. IEEE Trans Med Imag 22:965–972, 2003
14. Palti-Wasserman D, Brukstein AM, Beyar RP: Identifying and tracking a guide wire in the coronary arteries during angioplasty from X-ray images. IEEE Trans Biomed Eng 44:152–164, 1997
15. Takemura A, Harauchi H, Suzuki M, et al.: An algorithm for mapping the catheter tip position on a fluorograph to the three-dimensional position in magnetic resonance angiography volume data. Phys Med Biol 48:2697–2711, 2003
16. Sen A, Lan L, Doi K, et al.: Quantitative evaluation of vessel tracking techniques on coronary angiograms. Med Phys 26:698–706, 1999